

## Supramolecular Chemistry

DOI: 10.1002/ange.200602870

## Induction of Liquid Crystallinity by Self-Assembled Molecular Boxes

Alessio Piermattei, Marcel Giesbers,  
Antonius T. M. Marcelis, Eduardo Mendes,  
Stephen J. Picken, Mercedes Crego-Calama,\* and  
David N. Reinhoudt\*

The self-assembly of small molecular building blocks into supramolecular aggregates through noncovalent interactions has been used extensively for the formation of nanoscale structures.<sup>[1]</sup> For self-organization into highly ordered nano-architectures, the building blocks require well-defined structures with high thermodynamic stabilities.<sup>[2]</sup> Hydrogen bonding is a powerful tool for the construction of such structures, owing to its directional and dynamic nature,<sup>[3]</sup> and its capability for error correction.<sup>[4]</sup> A variety of liquid-crystalline materials<sup>[5]</sup> have been prepared by self-assembly through

hydrogen-bond formation.<sup>[6]</sup> Rodlike<sup>[7]</sup> and disklike<sup>[8,9]</sup> low-molecular-weight complexes, and polymers<sup>[10]</sup> with side-chain,<sup>[11]</sup> main-chain,<sup>[12]</sup> network, host-guest<sup>[9,13]</sup> arrangements, and single building blocks<sup>[14]</sup> have been reported.

The shape of the mesogenic molecule is one of the factors that determine the packing and order in the liquid-crystalline phase. Recently, unconventional shapes, such as bananas,<sup>[15]</sup> dendrons,<sup>[16]</sup> cones,<sup>[5]</sup> shuttlecocks,<sup>[5]</sup> rod-dendrons,<sup>[5]</sup> and rings<sup>[5]</sup> have been reported. The self-assembly of these unconventional mesogenic supramolecules has produced new phases of supramolecular liquid crystals.<sup>[17]</sup> To our knowledge, there have been no reports of hydrogen-bonded 3D nano-objects composed of different building blocks with the capability to form liquid crystals.


Herein, we report the first example of a liquid-crystalline material based on the self-organization of self-assembled molecular boxes. Each box consists of two rosette motifs connected through three calix[4]arene dimelamine molecules (**1**). The circular motifs (rosettes)<sup>[18]</sup> are formed by hydrogen bonding between the melamine moieties of **1** and a barbituric or cyanuric acid (Figure 1). The mesogenic double-rosette assemblies **1**<sub>3</sub>·(DEB)<sub>6</sub> (DEB = 5,5-diethylbarbituric acid) and **1**<sub>3</sub>·(BuCYA)<sub>6</sub> (BuCYA = *N*-butylcyanuric acid) form spontaneously upon mixing **1** with 2 equiv of either DEB or BuCYA in an apolar solvent (Figure 1).<sup>[19]</sup> The assemblies, which are held together by 36 hydrogen bonds, are thermodynamically stable, even at a concentration of 5 μM.<sup>[20]</sup> The calix[4]arene dimelamine **1** was functionalized with octadecyl chains to promote the self-organization of the double-rosette assemblies into a liquid-crystalline phase. The long alkyl chains are connected to the terminal benzamide moieties of **1** to prevent their interference with the network of hydrogen bonds that holds the double rosette together.<sup>[21]</sup>

The formation of the self-assembled mesogens was confirmed by <sup>1</sup>H NMR spectroscopy in solution (Figure 2). The signals assigned to the imide protons (a, b) of DEB and BuCYA at δ<sub>NH</sub> = 15–14 ppm are diagnostic of the formation of the assemblies; upon hydrogen-bond formation, the signals of these protons undergo a strong downfield shift (in free DEB, δ<sub>NH</sub> = 8.40 ppm; in free BuCYA, δ<sub>NH</sub> = 11.2 ppm).<sup>[19]</sup>

The thermal behavior of the assembly and of the isolated component **1** was determined by polarized optical microscopy (POM) and differential scanning calorimetry (DSC; Table 1). The DSC thermograms of the assemblies each exhibit two peaks associated with phase transitions. In the case of **1**<sub>3</sub>·(DEB)<sub>6</sub>, the first (low-temperature) peak is attributed to a reversible transition between an unidentified columnar (Col<sub>x</sub>) phase and a hexagonal columnar (Col<sub>h</sub>) phase. However, no differences were observed between the optical textures and the X-ray diffraction (XRD) patterns of the two phases. In the case of **1**<sub>3</sub>·(BuCYA)<sub>6</sub>, the first peak is attributed to a crystal–liquid crystal (Col<sub>h</sub> phase) transition. For both double-rosette assemblies, the second peak is attributed to a transition between a liquid-crystalline (Col<sub>h</sub>) and an isotropic phase. The thermotropic Col<sub>h</sub> phase exists over a wide temperature range for both assemblies (16–173 °C for **1**<sub>3</sub>·(DEB)<sub>6</sub>; 31–233 °C for **1**<sub>3</sub>·(BuCYA)<sub>6</sub>; Table 1). The thermal stability of the liquid-crystalline phase is remarkable, considering the dimensions (1.2 nm in height; 3.3 nm in

[\*] A. Piermattei, Dr. M. Crego-Calama, Prof. D. N. Reinhoudt  
Laboratory of Supramolecular Chemistry & Technology  
MESA<sup>+</sup> Institute for Nanotechnology  
University of Twente  
P.O. Box 217, 7500AE Enschede (The Netherlands)  
Fax: (+31) 534-894-645  
E-mail: m.cregocalama@utwente.nl  
d.n.reinhoudt@utwente.nl

Dr. M. Giesbers, Dr. A. T. M. Marcelis  
Laboratory of Organic Chemistry  
Wageningen University  
P.O. Box 8026, 6700EG Wageningen (The Netherlands)  
Dr. E. Mendes, Prof. S. J. Picken  
Nanostructured Materials (NSM-DCT)  
Faculty of Applied Sciences  
Julianalaan 136, 2628BL Delft (The Netherlands)

 Supporting information for this article (Experimental Section) is available on the WWW under <http://www.angewandte.org> or from the author.

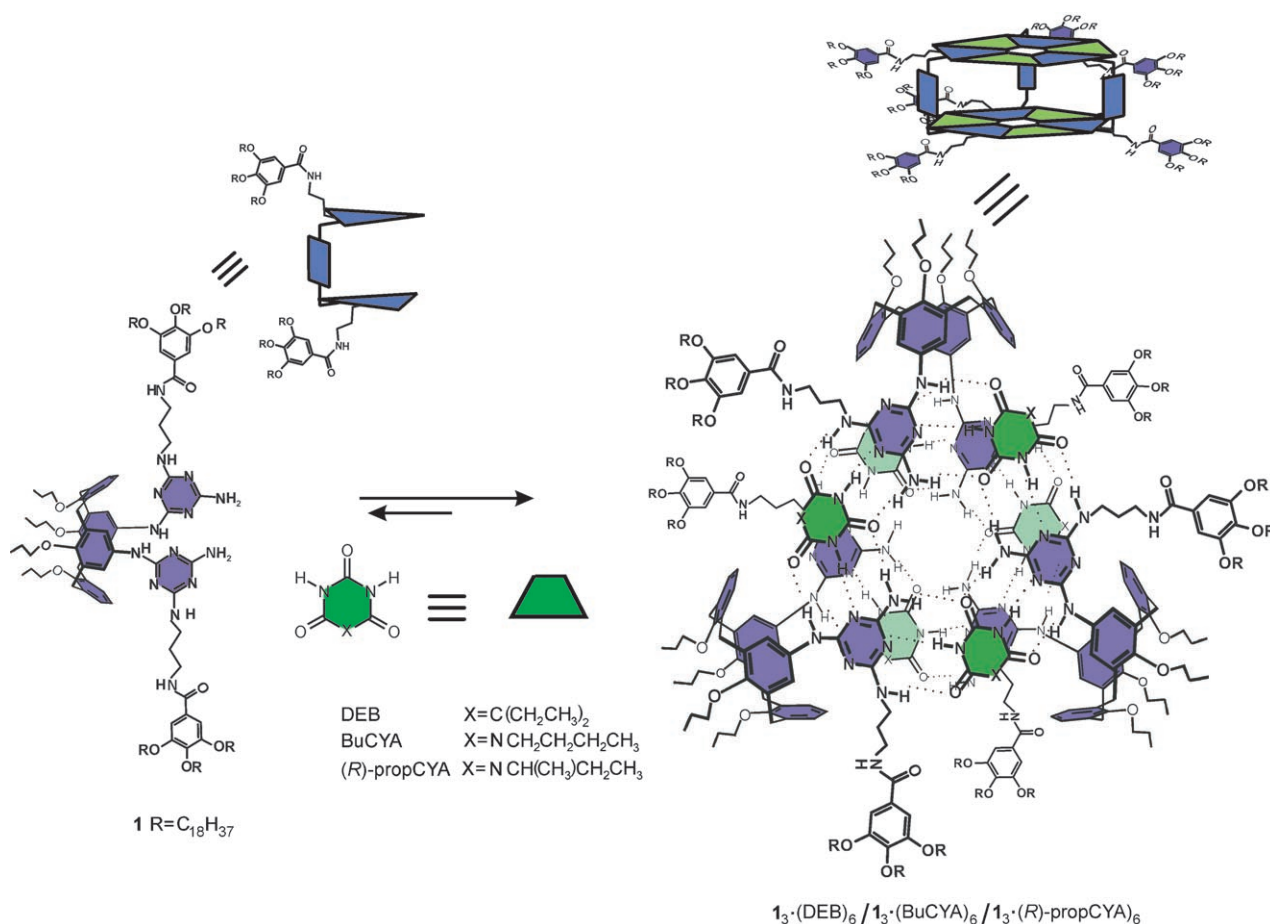


Figure 1. Self-assembly of  $1_3 \cdot (DEB)_6$ ,  $1_3 \cdot (BuCYA)_6$ , and  $1_3 \cdot ((R)\text{-propCYA})_6$ .

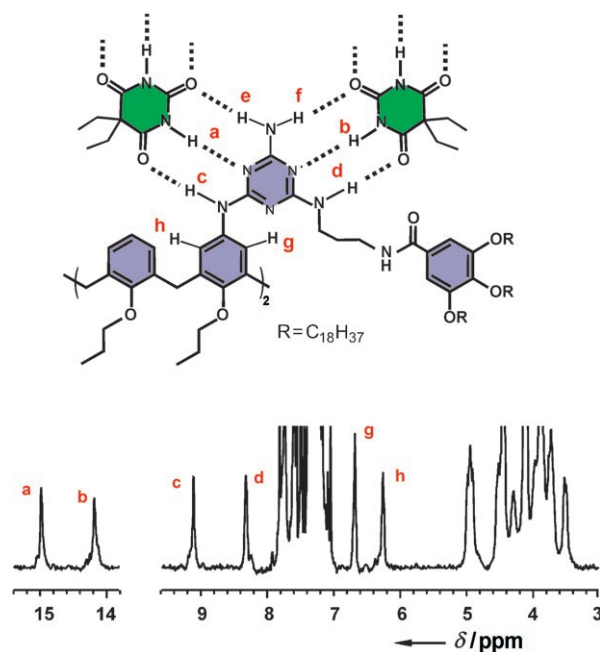


Figure 2. Sections of the  $^1\text{H}$  NMR spectrum (400 MHz) of  $1_3 \cdot (DEB)_6$  (1 mM in  $[\text{D}_8]\text{toluene}$ ) at 298 K.

Table 1: Thermal properties of **1**,  $1_3 \cdot (DEB)_6$ , and  $1_3 \cdot (BuCYA)_6$ .

Compound	Phase transition <sup>[a]</sup>				
<b>1</b>	Cr	17	(59.8)	Iso	
$1_3 \cdot (DEB)_6$	Col <sub>x</sub>	16	(18.7)	Col <sub>h</sub>	173 (35.0)
$1_3 \cdot (BuCYA)_6$	Cr	31	(167.5)	Col <sub>h</sub>	233 (70.1)

[a] Phase-transition temperatures  $^{\circ}\text{C}$  and enthalpy changes  $[\text{kJ mol}^{-1}]$  (in parentheses); Cr = crystalline phase, Col<sub>x</sub> = unidentified columnar phase, Col<sub>h</sub> = hexagonal columnar phase, Iso = isotropic phase.

width) and the noncovalent nature (12 DAD·ADA hydrogen bonds; D = donor, A = acceptor) of the double-rosette assembly.<sup>[19]</sup> In contrast, the DSC thermogram of **1** exhibits only one peak. This peak is attributed to a transition between a crystalline phase and an isotropic phase on the basis of POM, which reveals the spherulite texture of the crystalline phase. It is remarkable that the liquid-crystalline phase is observed for the double-rosette assemblies, even though none of the isolated building blocks are mesogenic.

To exclude the possibility of thermal degradation of the double-rosette assemblies during the heating process, circular dichroism (CD) studies on thin layers of the optically active assembly  $1_3 \cdot ((R)\text{-propCYA})_6$  ((R)-propCYA = *N*-(*R*)-1-methylpropyl]cyanuric acid) were performed (not

shown).<sup>[20,22,23]</sup> The optically active double-rosette assemblies (with *P* or *M* helicity) exhibit a very strong induced CD signal at a wavelength of 350–250 nm,<sup>[20]</sup> owing to the dissymmetric arrangement of the many chromophoric units, whereas the building block **1** is nearly CD inactive. The intensity of the CD signal of **1**<sub>3</sub>·((*R*)-propCYA)<sub>6</sub> does not decrease after several thermal cycles, evidencing the high thermal stability of the assembly.

POM suggests that the liquid-crystalline phase of the assemblies is a columnar mesophase: a mosaic texture showing birefringent areas is observed for **1**<sub>3</sub>·(DEB)<sub>6</sub> and **1**<sub>3</sub>·(BuCYA)<sub>6</sub> after cooling from the isotropic melt (Figure 3).

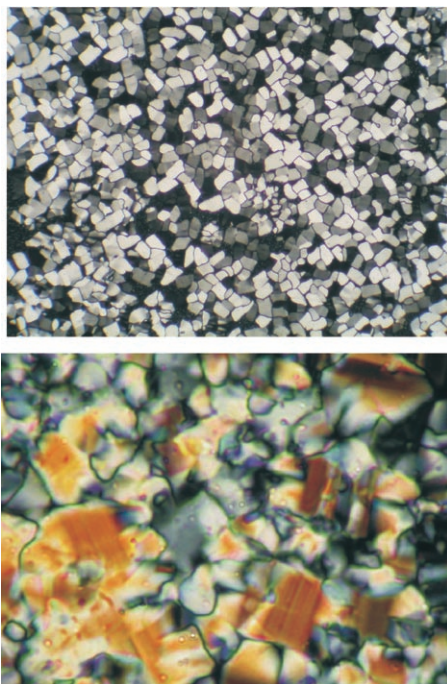


**Figure 3.** POM images of **1**<sub>3</sub>·(DEB)<sub>6</sub> at 120 °C (top) and of **1**<sub>3</sub>·(BuCYA)<sub>6</sub> at 180 °C (bottom).

Note that the assemblies **1**<sub>3</sub>·(DEB)<sub>6</sub> and **1**<sub>3</sub>·(BuCYA)<sub>6</sub> have very different isotropization temperatures ( $\Delta T_{\text{iso}} = 60$  °C; Table 1). Melamines form stronger hydrogen bonds with cyanurates than with barbiturates,<sup>[24]</sup> resulting in the higher thermal stability of **1**<sub>3</sub>·(BuCYA)<sub>6</sub>. Furthermore, cyanuric acids have a nitrogen atom with trigonal coordination geometry at position 5 of the heterocycle. As a result, in **1**<sub>3</sub>·(BuCYA)<sub>6</sub>, the butyl substituent and the heterocycle are in the same plane. Consequently, the rosette faces of the assembly can be considered as flat surfaces, which allow efficient stacking in the columnar phase. In contrast, barbituric acids have a carbon atom with tetrahedral coordination geometry at the 5 position. As suggested by molecular simulation studies,<sup>[25]</sup> the ethyl substituents at this carbon atom point to the top and bottom faces of the double-rosette assembly, which may weaken the interaction between neighboring assemblies within the columns and contribute to a lower thermal stability.

The powder XRD pattern for the Col<sub>h</sub> phase of **1**<sub>3</sub>·(DEB)<sub>6</sub> is shown in Figure 4. In the small-angle region, the relatively sharp reflections at 37.3 (100), 21.9 (110), 19.1 (200), and 14.0 Å (210) are characteristic of the hexagonal arrangement.

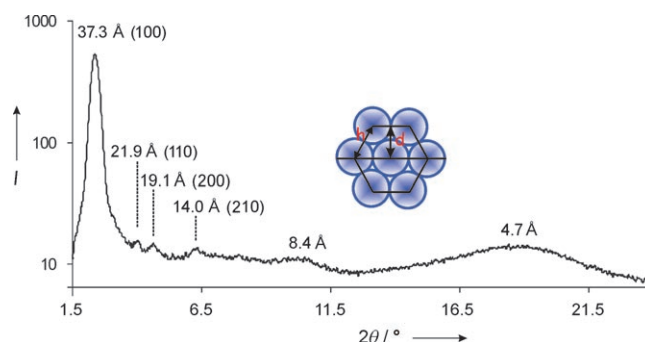


**Figure 4.** Powder XRD pattern of **1**<sub>3</sub>·DEB<sub>6</sub> at 120 °C, and schematic of the columnar organization in the Col<sub>h</sub> phase (see text for details).

A broad reflection at 8.4 Å corresponds to the distance between the bottom rosette faces of neighboring assemblies. In the wide-angle region, the diffuse halo near 4.7 Å arises from the disordered terminal alkyl chains and is characteristic of their liquid-like arrangement.

The double rosettes stack in an ordered columnar fashion. The driving force for the self-assembly of the columns is the nanoscale segregation of the double rosette cores and the lipophilic alkyl chains.<sup>[26]</sup> The intercolumn distance is  $h = 43.0$  Å (Figure 4).<sup>[27]</sup> A comparable distance was found by atomic force microscopy (AFM) for similar assemblies.<sup>[28]</sup> Their deposition onto highly ordered pyrolytic graphite (HOPG) showed that the double-rosette assemblies self-organize by face-to-face arrangement into rodlike structures. A hierarchical process leads from the self-assembly of double rosettes, to the assembly of the double rosettes into columns, and to the self-organization of the columns into a Col<sub>h</sub> liquid-crystalline phase, as demonstrated by XRD.

The powder XRD pattern of the Col<sub>h</sub> phase of **1**<sub>3</sub>·(BuCYA)<sub>6</sub> is very similar to that observed for **1**<sub>3</sub>·(DEB)<sub>6</sub>. This observation indicates that the side-chains of the cyanuric acid components do not interfere with the self-organization and packing, probably because the dimensions of the double-rosette scaffold are much larger than those of the side chains.<sup>[19]</sup>

Herein, we have demonstrated that the self-assembled double rosettes **1**<sub>3</sub>·(DEB)<sub>6</sub> and **1**<sub>3</sub>·(BuCYA)<sub>6</sub> are able to form liquid crystals. The strength of the hydrogen bonds within the double-rosette assemblies and the spatial disposition of the side chains of the barbituric and cyanuric acid derivatives are crucial factors for the stability of the mesophase. The lateral substituents on the double-rosette building blocks do not seem to affect the hierarchical organization of the mesophase. The remarkable thermal stability and the high degree of order of these mesophases, as well as the easy introduction of chemical diversity, make them a potentially good platform for the self-assembly of new nanomaterials.

Received: July 18, 2006

Published online: October 17, 2006

**Keywords:** hydrogen bonds · liquid crystals · nanotechnology · self-assembly · supramolecular chemistry

- [1] J.-M. Lehn, *Supramolecular Chemistry: Concepts and Perspectives*, VCH, Weinheim, **1995**.
- [2] D. N. Reinhoudt, *Supramolecular Materials and Technologies*, Wiley, Chichester, **1999**.
- [3] L. J. Prins, D. N. Reinhoudt, P. Timmerman, *Angew. Chem.* **2001**, *113*, 2446–2492; *Angew. Chem. Int. Ed.* **2001**, *40*, 2383–2426.
- [4] D. N. Reinhoudt, M. Crego-Calama, *Science* **2002**, *295*, 2403–2407.
- [5] T. Kato, N. Mizoshita, K. Kishimoto, *Angew. Chem.* **2006**, *118*, 44–74; *Angew. Chem. Int. Ed.* **2006**, *45*, 38–68.
- [6] C. M. Paleos, D. Tsiourvas, *Liq. Cryst.* **2001**, *28*, 1127–1161.
- [7] C. A. Schalley, *Adv. Mater.* **1999**, *11*, 1535–1537.
- [8] a) T. Kato, T. Matsuoka, M. Nishii, Y. Kamikawa, K. Kanie, T. Nishimura, E. Yashima, S. Ujiie, *Angew. Chem.* **2004**, *116*, 2003–2006; *Angew. Chem. Int. Ed.* **2004**, *43*, 1969–1972; b) J. van Gestel, A. R. A. Palmans, B. Titulaer, J. Vekemans, E. W. Meijer, *J. Am. Chem. Soc.* **2005**, *127*, 5490–5494; c) M. Suarez, J.-M. Lehn, S. C. Zimmerman, A. Skoulios, B. Heinrich, *J. Am. Chem. Soc.* **1998**, *120*, 9526–9532; d) G. Proni, G. P. Spada, G. Gottarelli, F. Ciuchi, P. Mariani, *Chirality* **1998**, *10*, 734–741.
- [9] J. Barberá, M. Bardají, J. Jiménez, A. Laguna, M. P. Martínez, L. Oriol, J. L. Serrano, I. Zaragozano, *J. Am. Chem. Soc.* **2005**, *127*, 8994–9002.
- [10] T. Kato, N. Mizoshita, K. Kanie, *Macromol. Rapid Commun.* **2001**, *22*, 797–814.
- [11] M. Ikeda, T. Nobori, M. Schmutz, J.-M. Lehn, *Chem. Eur. J.* **2005**, *11*, 662–668.
- [12] a) L. Brunsveld, E. W. Meijer, R. B. Prince, J. S. Moore, *J. Am. Chem. Soc.* **2001**, *123*, 7978–7984; b) J. Hirschberg, R. A. Koevoets, R. P. Sijbesma, E. W. Meijer, *Chem. Eur. J.* **2003**, *9*, 4222–4231.
- [13] a) S. Yagai, T. Nakajima, K. Kishikawa, S. Kohmoto, T. Karatsu, A. Kitamura, *J. Am. Chem. Soc.* **2005**, *127*, 11134–11139; b) F. Wurthner, S. Yao, B. Heise, C. Tschierske, *Chem. Commun.* **2001**, 2260–2261.
- [14] a) S. Bonazzi, M. M. Demorais, G. Gottarelli, P. Mariani, G. P. Spada, *Angew. Chem.* **1993**, *105*, 251–254; *Angew. Chem. Int. Ed. Engl.* **1993**, *32*, 248–250; b) M. Nishii, T. Matsuoka, Y. Kamikawa, T. Kato, *Org. Biomol. Chem.* **2005**, *3*, 875–880.
- [15] D. M. Walba, E. Korblova, R. Shao, J. E. MacLennan, D. R. Link, M. A. Glaser, N. A. Clark, *Science* **2000**, *288*, 2181–2184.
- [16] G. Ungar, Y. Liu, X. Zeng, V. Percec, W.-D. Cho, *Science* **2003**, *299*, 1208–1211.
- [17] V. Percec, M. Peterca, M. J. Sienkowska, M. A. Ilies, E. Aqad, J. Smidrkal, P. A. Heiney, *J. Am. Chem. Soc.* **2006**, *128*, 3324–3334.
- [18] C. T. Seto, G. M. Whitesides, *J. Am. Chem. Soc.* **1993**, *115*, 905–916.
- [19] P. Timmerman, R. H. Vreekamp, R. Hulst, W. Verboom, D. N. Reinhoudt, K. Rissanen, K. A. Udachin, J. Ripmeester, *Chem. Eur. J.* **1997**, *3*, 1823–1832.
- [20] L. J. Prins, C. Thalacker, F. Wurthner, P. Timmerman, D. N. Reinhoudt, *Proc. Natl. Acad. Sci. USA* **2001**, *98*, 10042–10045.
- [21] H. J. van Manen, V. Paraschiv, J. J. García-López, H. Schönherr, S. Zapotoczny, G. J. Vancso, M. Crego-Calama, D. N. Reinhoudt, *Nano Lett.* **2004**, *4*, 441–446.
- [22] L. J. Prins, J. Huskens, F. de Jong, P. Timmerman, D. N. Reinhoudt, *Nature* **1999**, *398*, 498–502.
- [23] The double-rosette assembly, in which the two melamine rings of each calix[4]arene molecule are antiparallel to one another, has  $D_2$  symmetry. In the absence of chiral centers, the assemblies are present as a racemic mixture of *P* and *M* helices. If one enantiomer of a barbituric or cyanuric acid with a chiral center is used in the self-assembly, only one diastereoisomer of the double rosette (of *P* or *M* helicity) is formed, which represents an induction of supramolecular chirality. The diastereoisomerism of the double-rosette assemblies allows them to be studied by CD.
- [24] A. G. Bielejewska, C. E. Marjo, L. J. Prins, P. Timmerman, F. de Jong, D. N. Reinhoudt, *J. Am. Chem. Soc.* **2001**, *123*, 7518–7533.
- [25] M. G. J. ten Cate, J. Huskens, M. Crego-Calama, D. N. Reinhoudt, *Chem. Eur. J.* **2004**, *10*, 3632–3639.
- [26] T. Kato, *Science* **2002**, *295*, 2414–2418.
- [27] The intercolumn distance  $h$  is calculated with the formula  $h = d / \cos(\pi/6)$ , where  $d$  is the distance between the (100) planes, which corresponds to the distance between adjacent layers of double-rosette columns.
- [28] H. A. Klok, K. A. Jolliffe, C. L. Schauer, L. J. Prins, J. P. Spatz, M. Möller, P. Timmerman, D. N. Reinhoudt, *J. Am. Chem. Soc.* **1999**, *121*, 7154–7155.